LIMNOLOGY and OCEANOGRAPHY

Promoting effects of aluminum addition on chlorophyll biosynthesis and growth of two cultured iron-limited marine diatoms

Linbin Zhou [iD],[1,2,3]* Fengjie Liu,[2,4] Eric P. Achterberg,[2] Anja Engel [iD],[2] Peter G.C. Campbell [iD],[5] Claude Fortin [iD],[5] Liangmin Huang,[1,3] Yehui Tan[1,3]*
[1]CAS Key Laboratory of Tropical Marine Bio-resources and Ecology, Guangdong Provincial Key Laboratory of Applied Marine Biology, South China Sea Institute of Oceanology, Chinese Academy of Sciences, Guangzhou, China
[2]Marine Biogeochemistry Division, GEOMAR Helmholtz Centre for Ocean Research, Kiel, Germany
[3]University of Chinese Academy of Sciences, Beijing, China
[4]Grantham Institute—Climate Change and the Environment, Department of Life Sciences, Imperial College London, London, UK
[5]Institut National de la Recherche Scientifique, Centre Eau Terre Environnement, Quebec, Canada

Abstract

Aluminum (Al) may play a role in the ocean's capacity for absorbing atmospheric CO_2 via influencing carbon fixation, export, and sequestration. Aluminum fertilization, especially in iron (Fe)-limited high-nutrient, low-chlorophyll ocean regions, has been proposed as a potential CO_2 removal strategy to mitigate global warming. However, how Al addition would influence the solubility and bioavailability of Fe as well as the physiology of Fe-limited phytoplankton has not yet been examined. Here, we show that Al addition (20 and 100 nM) had little influence on the Fe solubility in surface seawater and decreased the Fe bio-uptake by 11–22% in Fe-limited diatom *Thalassiosira weissflogii* in Fe-buffered media. On the other hand, the Al addition significantly increased the rate of chlorophyll biosynthesis by 45–60% for Fe-limited *T. weissflogii* and 81–102% for Fe-limited *Thalassiosira pseudonana*, as well as their cell size, cellular chlorophyll content, photosynthetic quantum efficiency (F_v/F_m) and growth rate. Under Fe-sufficient conditions, the Al addition still led to an increased growth rate, though the beneficial effects of Al addition on chlorophyll biosynthesis were no longer apparent. These results suggest that Al may facilitate chlorophyll biosynthesis and benefit the photosynthetic efficiency and growth of Fe-limited diatoms. We speculate that Al addition may enhance intracellular Fe use efficiency for chlorophyll biosynthesis by facilitating the superoxide-mediated intracellular reduction of Fe(III) to Fe(II). Our study provides new evidence and support for the iron–aluminum hypothesis.

Carbon dioxide removal is needed to achieve the target during this century of limiting average global warming to no more than 2°C above the pre-industrial level (IPCC 2022). The ocean is the largest active carbon reservoir, and it has a large potential to remove CO_2 from the atmosphere (GESAMP et al. 2019; Friedlingstein et al. 2022; Liu et al. 2022). Phytoplankton are an important factor in regulating the ocean's capacity for absorbing CO_2 from the atmosphere; however, their growth is limited in almost one third of the world's surface ocean by a limited supply of iron (Fe) (Moore et al. 2013; Browning and Moore 2023).

The Iron Hypothesis suggests that Fe fertilization in Fe-limited high-nutrient, low-chlorophyll (HNLC) regions such as the Southern Ocean will stimulate phytoplankton growth and draw down atmospheric CO_2 concentrations, and thereby cool the earth (Martin 1990; Martin et al. 1990). Artificial Fe fertilization experiments showed that Fe fertilization significantly stimulated the growth of marine phytoplankton, especially diatoms in the HNLC oceans (Boyd et al. 2007). However, in some of the experiments, most of the phytoplankton-made particulate organic carbon was remineralized in the upper ocean and released back into the atmosphere as CO_2.

Additional Supporting Information may be found in the online version of this article.

No significant Fe-induced increase in the carbon flux to the ocean depths (e.g., below the winter mixed layer) was detected in most of the 13 artificial Fe fertilization experiments (Martin et al. 2013; Yoon et al. 2018). In addition, the Fe use efficiencies (carbon export: Fe supply) of the artificial Fe fertilization trials were low at only about 1–10% of those observed for natural Fe fertilization (Blain et al. 2007; de Baar et al. 2008; Pollard et al. 2009). Note that natural Fe fertilization through dust deposition, sediment resuspension, river runoff, and hydrothermal venting provides the ocean not only with Fe but also with Al and other elements (Zhou et al. 2018b).

Recent studies suggest that Al may play an important role in the ocean carbon cycle by influencing Fe bioavailability, carbon fixation by marine phytoplankton, and organic matter decomposition (Zhou et al. 2021). For example, an early study showed that the presence of Al (500 nM) increased Fe uptake by the marine diatom *Thalassiosira weissflogii* (Santana-Casiano et al. 1997). It has been suggested that Al may facilitate the superoxide-mediated reduction of ferric Fe (Fe(III)) to ferrous Fe (Fe(II)) in vivo (Exley 2004; Mujika et al. 2011; Ruipérez et al. 2012). Zhou et al. (2018b) borrowed this idea and proposed that a similar process may occur in vitro, and thus increase the bioavailability of Fe to marine phytoplankton. Moreover, Al may replace and liberate Fe associated with ligands and colloids in seawater, and hence alter the solubility and speciation of Fe (M. Gledhill pers. comm.). A number of studies have reported that the presence of Al favors the growth and increases the net carbon fixation of marine phytoplankton such as diatoms (Stoffyn 1979; Zhou et al. 2016, 2021) and cyanobacteria (Shi et al. 2015; Liu et al. 2018; Zhou et al. 2018a). Moreover, Al has long been known to decrease the dissolution rate of diatom frustules (Lewin 1961; Dixit et al. 2001; Tian et al. 2023). Aluminum addition at environmentally relevant levels has also been reported to decrease the decomposition rates of marine diatoms (Zhou et al. 2021) and decaying cyanobacterium *Trichodesmium* (Zhou et al. 2023b). Aluminum may also contribute to the long-term preservation and sequestration of carbon in microfossils and sediments (Blattmann et al. 2019; Hemingway et al. 2019; Anderson et al. 2020).

On the basis of the knowledge of the effects of Al on carbon fixation by marine phytoplankton, carbon export, and carbon sequestration, the iron–aluminum hypothesis was proposed to suggest that the inputs of Al as well as Fe through dust deposition to the Southern Ocean played an important role in the glacial–interglacial climate cycles (Martin 1990; Zhou et al. 2018b). As a result, Al fertilization in the ocean, especially in Fe-limited HNLC regions such as the Southern Ocean, has been proposed as a potential CO$_2$ removal strategy to cope with global warming (Zhou et al. 2023a). Adding both Al and Fe to the HNLC oceans has been suggested to not only facilitate an increase in phytoplankton carbon fixation in the upper ocean but also enhance carbon export to and sequestration in the deep ocean (Zhou et al. 2018b, 2021). However,

how Al fertilization influences the growth of Fe-limited phytoplankton has not yet been examined. In addition, the potential effects of Al addition on the solubility of Fe in seawater and its uptake by marine phytoplankton under Fe-limited conditions remain unexplored. We hypothesize that Al addition may stimulate diatom growth under Fe-limited conditions by influencing Fe bioavailability.

To test the hypothesis, using a Fe radioisotope (^{55}Fe), we examined the influences of Al addition on the solubility of Fe in natural seawater and the Fe uptake rate by the marine diatom *T. weissflogii*. We also investigated the responses of two Fe-limited marine diatoms (*T. weissflogii* and *T. pseudonana*) to Al enrichment (20 and 100 nM) under Fe-limited and Fe-sufficient conditions. The diatom responses with respect to chlorophyll biosynthesis, cellular chlorophyll content, photosynthetic quantum efficiency (F_v/F_m, indicating potential maximal photosynthesis performance), and growth rates based on cell abundance and cell biovolume were monitored.

Materials and methods

Cultures of marine diatoms

Axenic cultures of *T. weissflogii* and *T. pseudonana* were obtained from the National Center for Marine Algae and Microbiota—Bigelow Laboratory for Ocean Sciences (USA). The cultures were maintained in a Fe-limited Aquil* medium (Supporting Information Table S1) contained in polycarbonate bottles at 20°C under constant illumination (100 μmol m^{-2} s^{-1}).

The Fe-limited Aquil* medium was prepared with filtered North Atlantic surface seawater, using a 0.8/0.2-μm filter cartridge (AcroPak 500, Pall). The background metal concentrations in the filtrate (mean $\pm$ SD, $n = 16$–21) were 2.7 $\pm$ 0.8 nM Al, 0.62 $\pm$ 0.04 nM manganese, 0.35 $\pm$ 0.08 nM Fe, 0.034 $\pm$ 0.002 nM cobalt, 2.75 $\pm$ 0.08 nM nickel, 0.92 $\pm$ 0.05 nM copper, and 0.48 $\pm$ 0.07 nM zinc. Filtered seawater and polycarbonate bottles were sterilized by microwaving. Stock solutions (1000×) of macronutrients, micronutrients, and vitamins were sterilized by 0.2-μm syringe filtration (Sunda et al. 2005). The stock solutions were added to the sterilized filtered seawater in polycarbonate bottles to prepare the Fe-limited Aquil* medium with macronutrients of 100 μM nitrate, 100 μM silicic acid, and 10 μM phosphate, micronutrients of 40 nM Fe, 79.7 nM zinc, 121 nM manganese, 50.5 nM cobalt, 19.6 nM copper, and 10 nM selenium buffered with 100 μM ethylenediaminetetraacetate (EDTA), and vitamins of 0.55 μg L^{-1} vitamin B$_{12}$, 0.50 μg L^{-1} biotin, and 0.10 mg L^{-1} thiamine (Supporting Information Table S1).

Experimental designs
Influence of Al addition on the concentration of dissolved Fe (Fe solubility) in natural seawater

To test whether the presence of Al influences the concentration of dissolved Fe (i.e., Fe solubility) in seawater, the changes in dissolved Fe (< 0.22 μm) labeled with ^{55}Fe were

monitored in filtered North Atlantic surface seawater enriched with different Al concentrations (0, 20, and 100 nM). Specifically, 10 μL ^{55}FeCl$_3$ stock solution (2.083×10^{13} Bq mol^{-1}, or 49.93 Ci g^{-1} Fe in 1.6 mM HCl) was added to 100 mL filtered Atlantic surface seawater, yielding a concentration of 3.6 nM Fe. After being thoroughly mixed, 10-mL aliquots were transferred into nine 15-mL acid-clean Teflon tubes. Six 0.5-mL aliquots were transferred into six liquid scintillation vials for analysis of the initial counts of ^{55}Fe. For preparing the treatments of the control, +20 nM Al, and +100 nM Al, we added 10 μL of 0.01 M HCl solution, 20 and 100 μM AlCl$_3$ (trace metal basis 99.999%, Sigma-Aldrich) stock solutions prepared in 0.01 M HCl (Optimum grade, Fisher Scientific) separately to the 10 mL seawater samples in the 15-mL Teflon tubes. The addition of the equivalent of only 1 mL of 0.01 M HCl to 1000 mL of seawater did not influence the pH of seawater (< 0.01 pH units). Three replicates were prepared for each treatment. The final pH was 8.10 for each treatment.

The experimental tubes were set in darkness at room temperature (20°C). Dissolved Fe in the seawater was sampled on Days 0 (within 30 min from the beginning of the experiment), 1, 4, 8, 24, and 40. The seawater in the Teflon tubes was thoroughly mixed before sampling and then an aliquot of 0.5 mL seawater was syringe-filtered (0.22 μm, Millex® GP filter units) directly into a 5-mL scintillation vial. The filtered samples were used for determining dissolved Fe labeled with ^{55}Fe. The precise volume of the filtered seawater in each vial was measured by weighing the vial before and after the addition of the sample, using a high-precision electronic balance ($\pm$ 0.1 mg).

Two milliliters of scintillation cocktail (Ultima Gold AB, PerkinElmer) were added to each scintillation vial, thoroughly mixed, and allowed to stand overnight before analyzing for ^{55}Fe counts by using a liquid scintillation analyzer (Tri-Carb 2910 TR, PerkinElmer).

Influence of Al addition on Fe uptake rate by Fe-limited *T. weissflogii*

To examine the effects of Al on Fe uptake by marine diatoms, ^{55}Fe was used in Fe uptake experiments with Fe-limited *T. weissflogii*.

The filtered North Atlantic surface seawater was used for preparing the exposure media. No macronutrients (e.g., silicic acid, phosphate, and nitrate) or vitamins were added to the medium. Micronutrients including 40 nM Fe and other trace metals were added following the recipe for Aquil* medium and buffered with 100 μM EDTA. A 100-μL portion of the ^{55}FeCl$_3$ stock solution was then added to 500 mL of the medium, yielding a final total concentration of 47 nM Fe (54 pM [Fe′]). The control, +20 nM Al, +100 nM Al treatments were prepared using the same Al stock solutions as mentioned above. The media were allowed to stand overnight before use to reach chemical equilibrium. The final pH was 8.10 for each treatment.

The concentrations of dissolved inorganic iron [Fe′] in the media were calculated using the temperature-adjusted dissociation factors from Sunda and Huntsman (2003) and the equation from Sunda et al. (2005) (*see* details in Jabre and Bertrand 2020). The concentrations and speciation of dissolved Al and its influence on Fe speciation were calculated using the Visual MINTEQ model version 3.1 (Gustafsson 2020) and the seawater component according to Sunda et al. (2005) (Supporting Information Table S2).

T. weissflogii cells in the exponential growth phase cultured in Fe-limited Aquil* medium were collected onto acid-washed polycarbonate membrane filters (Millipore, 3 μm pore size, 47 mm diameter) by gravity filtration and rinsed three times with the filtered seawater. The cells on the membrane were re-suspended in the filtered seawater. Then 5 mL of the cell suspension was added to 500 mL exposure media with different concentrations of Al to reach a final density of 1.6×10^4 cells mL^{-1}. Three replicates were run for each treatment. The cells were incubated at 20°C under constant illumination (100 μmol m^{-2} s^{-1}). All the experiments and sampling operations were conducted in a clean laboratory (ISO 5).

Cell abundance and mean cell diameter (equivalent spherical diameter) were measured in the cell suspension with an electronic particle counter (Multisizer 2 Coulter Counter with a 100-μm aperture; Beckman).

Diatom cells were sampled at the time points of 23, 191, and 343 min for measuring cellular ^{55}Fe content. To measure cellular ^{55}Fe, diatom cells in 50-mL portions of each treatment were collected by filtration onto polycarbonate membrane filters (3 μm pore size, 25 mm diameter), soaked in 10 mL EDTA–oxalate washing reagent for 5 min and then rinsed three times with 5 mL filtered seawater to remove ^{55}Fe associated with cell walls (Tovar-Sanchez et al. 2003). The filter membrane with cells was transferred into a 20-mL scintillation vial, and a 5 mL scintillation cocktail (Ultima Gold AB, PerkinElmer) was added and thoroughly mixed, and allowed to stand overnight before analysis for ^{55}Fe counts using a liquid scintillation analyzer (Tri-Carb 2910 TR, PerkinElmer).

Influence of Al addition on the photosynthesis and growth of Fe-limited diatoms

To examine the effects of Al addition on chlorophyll biosynthesis, photosynthesis, and growth of diatoms, Fe-limited diatoms were transferred to Fe-limited and Fe-sufficient Aquil* media with different Al concentrations (0, 20, and 100 nM). The diatom responses in terms of in vivo chlorophyll, cell abundance, mean cell size, cellular chlorophyll content, photosynthetic quantum efficiency (F_v/F_m), and growth rate were monitored.

Specifically, the Fe-limited Aquil* medium was the same as the maintenance medium. The Fe-sufficient Aquil* medium was prepared by adding 500 nM Fe, while all other macronutrients, micronutrients, vitamins, and EDTA were the same as for the Fe-limited medium (Supporting Information Table S1).

The majority of the Fe in the media was chelated with EDTA, and only a small proportion was left in dissolved inorganic form (Sunda et al. 2005). The concentrations of dissolved inorganic Fe [Fe′] were 46 and 576 pM in the Fe-limited and Fe-sufficient media, respectively. Aluminum concentrations of 20 and 100 nM were set by adding the appropriate volumes of 20 and 100 μM AlCl$_3$ stock solutions to the experimental medium, respectively. Three replicates were set for each treatment. All the bottles and tubes used for preparing the reagents and solutions were acid-cleaned. All the media were prepared and allowed to sit overnight before use to reach chemical equilibrium.

Diatom cells in the exponential growth phase in 10 mL of the Fe-limited Aquil* medium were added to 100 mL samples of the experimental media. The initial cell densities were 6100 cells mL^{-1} for *T. weissflogii* and 6800 cells mL^{-1} for *T. pseudonana*. The experimental cultures were kept at 20°C under constant illumination (100 μmol m^{-2} s^{-1}). All the sampling and operations were done aseptically in a laminar flow hood in a clean laboratory (ISO 5).

Cell abundance, mean cell diameter, in vivo chlorophyll, and photosynthetic quantum efficiency (F_v/F_m) of the diatoms for each treatment were monitored three times within 8 h. Cell abundance and mean cell diameter were determined with an electronic particle counter (Multisizer 2 Coulter Counter with a 100-μm aperture; Beckman). Photosynthetic quantum efficiency (F_v/F_m) indicating potential maximum photosynthetic performance and in vivo chlorophyll were measured by using Fast Repetition Rate Fluorometry (FastOcean Sensor).

Cell biovolume was calculated by using the cell diameter. Growth rates based on the changes in cell abundance, cell biovolume, and in vivo chlorophyll were calculated as the linear regression slope of the natural logarithms of cell abundance, cell biovolume, and in vivo chlorophyll concentration with incubation time, respectively. The growth rates based on in vivo chlorophyll indicate the net chlorophyll biosynthesis rates. Cellular chlorophyll content and chlorophyll per biovolume were calculated by dividing in vivo chlorophyll concentration by cell abundance and cell biovolume, respectively.

Data analysis

One-way ANOVA was used to compare mean values among treatments. The values included the concentration of ^{55}Fe-labeled dissolved Fe in seawater, ^{55}Fe-labeled diatom cellular Fe, in vivo chlorophyll concentration, cell abundance, cell biovolume, mean cell diameter, chlorophyll per biovolume, cellular chlorophyll content, F_v/F_m, and growth rates. Least-significant-difference pairwise comparisons followed the one-way ANOVA and independent *t*-tests were used to compare mean values between the control and Al-enriched treatments. Analysis of covariance (ANCOVA) was used to compare the Fe uptake rates. If the variance homogeneity hypothesis was violated, a nonparametric test (Kruskal–Wallis test) was used to compare mean values among treatments. One-way repeated-measures ANOVA with Mauchly's test of sphericity was conducted to compare mean values of in vivo chlorophyll concentration, chlorophyll per biovolume, cellular chlorophyll content, and F_v/F_m among treatments during the incubation experiments under Fe-limited conditions. The statistical analyses were conducted by using the R version 4.2.3 software (R Core Team 2023).

Results

Influence of Al on the concentration of dissolved Fe (Fe solubility) in North Atlantic surface seawater

As indicated in Fig. 1, after the addition of ^{55}FeCl$_3$ to pre-filtered North Atlantic surface seawater, dissolved Fe (< 0.22 μm) in all the treatments decreased quickly from about 2.6 to 1.8 nM over the first 8 d. The dissolved Fe concentrations remained relatively stable at around 2 nM after Day 8. This behavior of Fe was not influenced in a consistent manner by the addition of Al. Relatively higher concentrations of dissolved Fe in the Al-enriched treatments compared to the control were observed only on Day 4 (ANOVA, $p = 0.09$) and Day 24 (ANOVA, $p > 0.1$). There were no significant differences in dissolved Fe concentrations among treatments at the other sampling time points (Fig. 1). Some of the Fe in the fraction of < 0.22 μm may be in colloidal form. The results indicate that the presence of Al did not have a significant effect on the concentration of dissolved Fe or Fe solubility in our sample of Atlantic seawater.
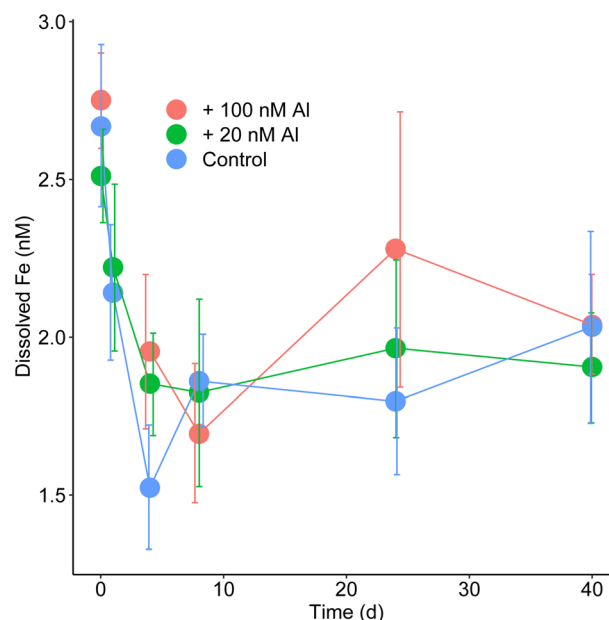

Fig. 1. Changes of dissolved iron (Fe) (< 0.22 μm) with time in North Atlantic surface seawater enriched with different concentrations of aluminum (Al). The error bars represent standard deviations (n = 3). Note that the error bars are dodged for better visibility.

Iron uptake rates by Fe-limited *T. weissflogii* in the presence of Al

Cellular ^{55}Fe content increased linearly with exposure time (Fig. 2; Supporting Information Fig. S1), indicating significant ($p < 0.001$) uptake of Fe by the diatom in all treatments. Higher cellular Fe was observed in the treatments enriched with higher concentrations of Al at the first time point (Supporting Information Fig. S1), but at the subsequent time points cellular Fe was higher in the control exposure. Indeed, cellular ^{55}Fe increased more rapidly in the control than in the Al-enriched treatments, and the control cells had a higher cellular ^{55}Fe than the Al-treated cells at the end of the uptake experiments.

As a result, the diatom cells in the control treatment had a higher overall Fe uptake rate than those in the Al-enriched treatments (Fig. 2; Supporting Information Table S3) (ANCOVA, $p < 0.001$). Compared to the control, the Fe uptake rates were lower by 22% and 11% in the treatments enriched with 20 and 100 nM Al, respectively.

Effects of Al addition on the accumulation of diatom biomass

The diatom biomass in terms of in vivo chlorophyll, cell abundance, and cell biovolume all increased with incubation time. Ample Fe supply in the Fe-sufficient media (576 pM [Fe′]) compared to the Fe-limited media (46 pM [Fe′]) resulted in significantly higher diatom biomass accumulation ($p < 0.001$)
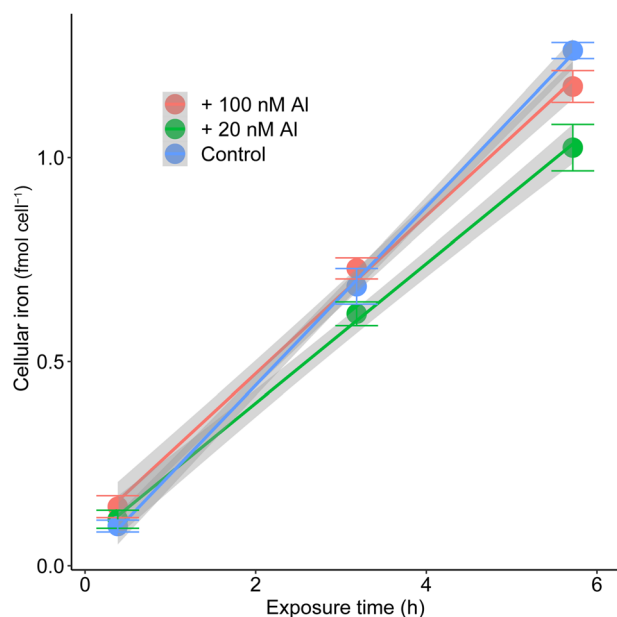

Fig. 2. Cellular ^{55}Fe in *Thalassiosira weissflogii* vs. exposure time in seawater with 47 nM ^{55}Fe buffered by 100 μM EDTA (i.e., 54 pM [Fe′]) and with different concentrations of aluminum (Al). The error bars represent standard deviations (n = 3). The regression lines show the linear increases in cellular Fe with exposure time. The gray zones indicate 95% confidence intervals of the regression lines.

(Fig. 3; Table 1). Aluminum addition under Fe-limited conditions also enhanced the accumulation of diatom biomass (Fig. 3).

Significantly higher in vivo chlorophyll concentrations were observed for the two diatom species in the Al-enriched treatments compared to the control under Fe-limited conditions (ANOVA, $p < 0.001$) (Fig. 3a,c). Higher in vivo chlorophyll concentrations in the Al-enriched treatments compared to the control occurred after 2 h of incubation, and the differences between the control and the Al-enriched treatments increased over incubation time (repeated-measures ANOVA, $p < 0.01$; Mauchly's test of sphericity, $p > 0.05$) (Fig. 3a,c). Aluminum addition under Fe-sufficient conditions did not change the in vivo chlorophyll concentration of the two diatom incubations (ANOVA, $p > 0.1$) (Fig. 3b,d).

Aluminum addition under Fe-limited conditions did not significantly change the final cell abundance and cell biovolume of *T. weissflogii* (ANOVA, $p > 0.1$) (Fig. 3e,i). In contrast, higher cell abundances and cell biovolumes of *T. weissflogii* were observed in treatments enriched with higher concentrations of Al under Fe-sufficient conditions (ANOVA, $p < 0.05$; Kruskal–Wallis test, $p < 0.01$) (Fig. 3f,j).

For the diatom *T. pseudonana*, higher cell abundances were observed in treatments enriched with higher concentrations of Al under both Fe-limited (ANOVA, $p < 0.001$) (Fig. 3g) and Fe-sufficient conditions (ANOVA, $p = 0.004$) (Fig. 3h). Aluminum addition also significantly increased the total cell biovolume of *T. pseudonana* under both Fe-limited and Fe-sufficient conditions (ANOVA, $p < 0.001$) (Fig. 3k,l).

Effects of Al addition on the diatom cellular chlorophyll content and photosynthetic efficiency under Fe-limited conditions

The results showed that Al addition in Fe-limited media (46 pM [Fe′]) not only increased in vivo chlorophyll concentrations in the diatom cultures (Fig. 3a,c) but also significantly (ANOVA, $p < 0.01$) increased diatom cellular chlorophyll content and photosynthetic quantum efficiency (Fig. 4e,g,i,k,m,o; Table 1).

Sufficient Fe supply led to significantly higher mean cell size, chlorophyll per biovolume, cellular chlorophyll content, and photosynthetic quantum efficiency (F_v/F_m) of the diatoms in the Fe-sufficient media compared to the Fe-limited media at the end of incubation (ANOVA, $p < 0.001$) (Fig. 4; Table 1). The mean cell diameter, chlorophyll per unit biovolume, cellular chlorophyll content, and F_v/F_m of *T. weissflogii* increased by 0.9% ($p < 0.001$), 7.6% ($p = 0.001$), 10.8% ($p < 0.001$), and 20.6% ($p < 0.001$) in the Fe-sufficient media, compared to the Fe-limited media, respectively. The same monitored parameters for *T. pseudonana* increased by 1.4% ($p < 0.001$), 44.5% ($p < 0.001$), 50.5% ($p < 0.001$), and 11.6% ($p < 0.001$) in the Fe-sufficient media, compared to the Fe-limited media, respectively (Fig. 4).
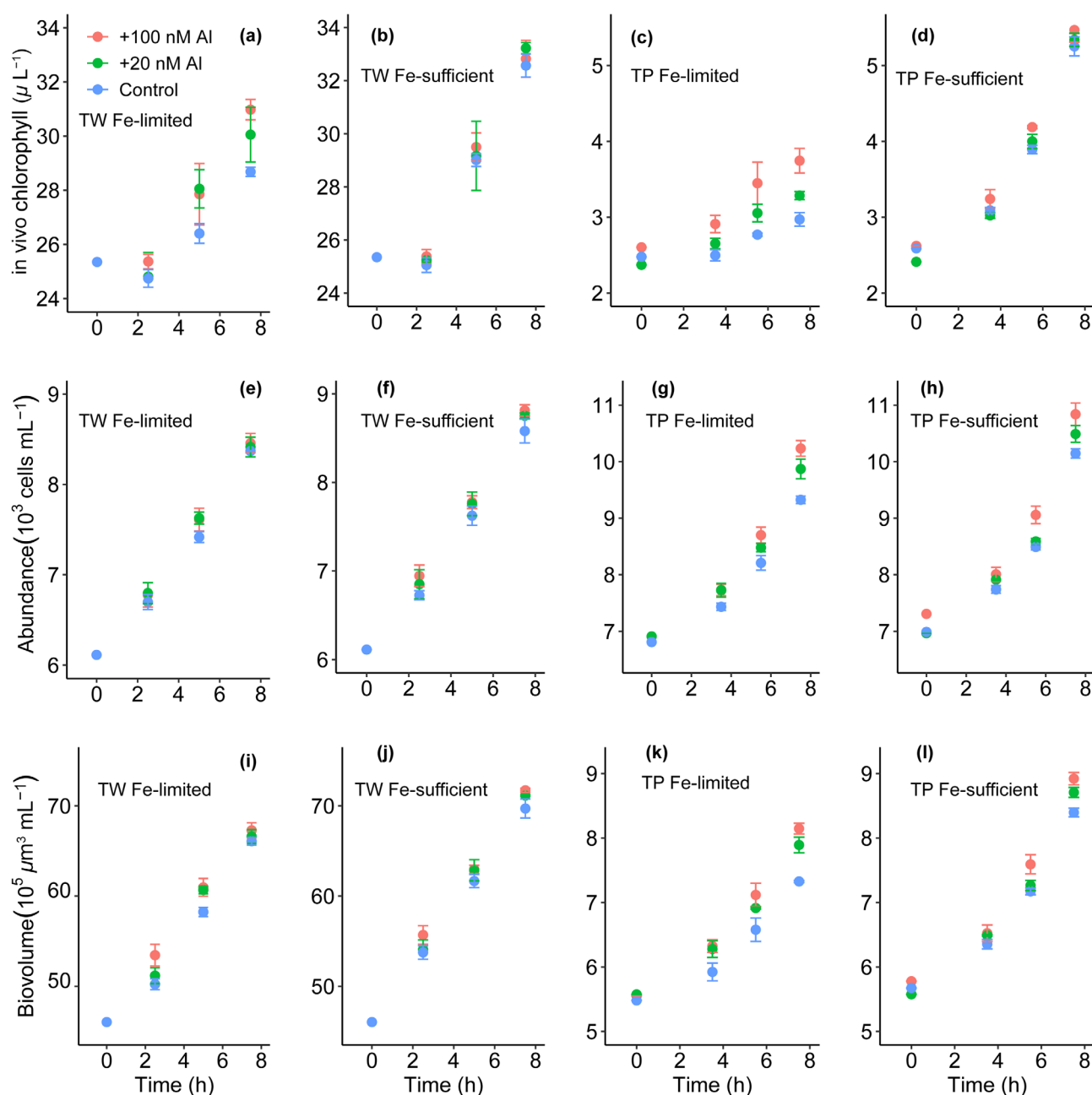
Fig. 3. Effects of aluminum (Al) addition on biomass accumulation of two diatoms (*Thalassiosira weissflogii* (TW) and *T. pseudonana* (TP)) in Fe-limited (46 pM [Fe']) and Fe-sufficient (576 pM [Fe']) Aquil* media. The error bars represent standard deviations (n = 3).

Aluminum addition under Fe-limited conditions increased the mean cell size, chlorophyll per biovolume, cellular chlorophyll content, and photosynthetic quantum efficiency (F_v/F_m) of the diatoms (Fig. 4). Specifically, Al addition to Fe-limited media increased the chlorophyll content per biovolume by 4.0–6.1% for *T. weissflogii* (Kruskal–Wallis test, $p = 0.061$) (Fig. 4e), and 2.7–13.3% for *T. pseudonana* (ANOVA, $p = 0.006$) (Fig. 4g). Aluminum addition to Fe-limited media also increased the cellular chlorophyll content by 4.2–6.9%

for *T. weissflogii* (Kruskal–Wallis test, $p = 0.051$) (Fig. 4i) and by 4.5–14.8% for *T. pseudonana* (ANOVA, $p = 0.006$) (Fig. 4k). Aluminum addition also increased the mean cell diameter by 0.1–0.3% for *T. weissflogii* (ANOVA, $p > 0.1$) and by 0.6–0.8% for *T. pseudonana* (ANOVA, $p < 0.01$) in the Fe-limited media (Fig. 4a,c).

Consistent with the increase in diatom cellular chlorophyll content in Fe-limited media, the diatom F_v/F_m value in the Al-enriched treatments increased by 12.0–12.7% for *T. weissflogii*

Table 1. Effects of aluminum (Al) addition on the biomass accumulation, mean cell size, chlorophyll (Chl) biosynthesis rate, cellular Chl content, photosynthetic quantum efficiency (F_v/F_m), and growth rates of two marine diatoms (*Thalassiosira weissflogii* and *Thalassiosira pseudonana*) in Fe-limited (46 pM [Fe']) and Fe-sufficient (576 pM [Fe']) Aquil* media. The data are expressed as mean ± standard deviations ($n = 3$). The symbols #, *, and ** indicate nearly significant ($0.05 < p < 0.1$), significant ($p < 0.05$), and highly significant ($p < 0.01$) differences compared to the controls (46 or 576 pM [Fe']), respectively.

|	Parameters	46 pM [Fe']	46 pM [Fe'] + 20 nM Al	46 pM [Fe'] + 100 nM Al	576 pM [Fe']	576 pM [Fe'] + 20 nM Al	576 pM [Fe'] + 100 nM Al	46 vs. 576 pM [Fe'], significance
T. Weissflogii	In vivo Chl (μg L⁻¹)	28.68 ± 0.17	30.05 ± 1.01*	30.98 ± 0.38**	32.57 ± 0.43	33.22 ± 0.21	32.82 ± 0.70	$p < 0.001$
	Cell abundance (10³ cells mL⁻¹)	8.37 ± 0.00	8.41 ± 0.11	8.46 ± 0.11	8.58 ± 0.13	8.75 ± 0.03*	8.81 ± 0.06**	$p < 0.05$
	Cell biovolume (10⁵ μm³ mL⁻¹)	66.07 ± 0.41	66.60 ± 0.77	67.28 ± 0.84#	69.70 ± 0.00	71.13 ± 0.10*	71.72 ± 0.24**	$p < 0.001$
	Mean cell diameter (μm)	11.48 ± 0.02	11.48 ± 0.01	11.50 ± 0.03	11.58 ± 0.02	11.58 ± 0.01	11.58 ± 0.02	$p < 0.001$
	Cellular Chl content (pg cell⁻¹)	3.43 ± 0.02	3.57 ± 0.14*	3.66 ± 0.08**	3.80 ± 0.01	3.08 ± 0.02	3.72 ± 0.10	$p < 0.001$
	Chl per biovolume (g L⁻¹)	4.34 ± 0.04	4.51 ± 0.18*	4.60 ± 0.07**	4.67 ± 0.01	4.67 ± 0.03	4.58 ± 0.09	$p = 0.001$
	F_v/F_m	0.388 ± 0.072	0.435 ± 0.003#	0.438 ± 0.003#	0.468 ± 0.002	0.474 ± 0.004	0.464 ± 0.003	$p < 0.001$
	Chl biosynthesis rate (h⁻¹)	0.0174 ± 0.0009	0.0253 ± 0.0062*	0.0278 ± 0.0025*	0.0359 ± 0.0018	0.0382 ± 0.0022	0.0370 ± 0.0024	$p < 0.001$
	Abundance-based growth rates (h⁻¹)	0.0418 ± 0.0006	0.0429 ± 0.0012	0.0436 ± 0.0020	0.0457 ± 0.0011	0.0481 ± 0.0013*	0.0484 ± 0.0013*	$p = 0.004$
	Biovolume-based growth rates (h⁻¹)	0.0493 ± 0.0010	0.0511 ± 0.0011#	0.0508 ± 0.0015	0.0553 ± 0.0013	0.0582 ± 0.0008**	0.0581 ± 0.0008**	$p < 0.001$
T. Pseudonana	In vivo Chl (μg L⁻¹)	2.97 ± 0.09	3.29 ± 0.05**	3.74 ± 0.16**	5.25 ± 0.13	5.33 ± 0.090	5.47 ± 0.16#	$p < 0.001$
	Cell abundance (10³ cells mL⁻¹)	9.33 ± 0.07	9.87 ± 0.17**	10.23 ± 0.14**	10.15 ± 0.08	10.49 ± 0.15*	10.84 ± 0.20**	$p < 0.001$
	Cell biovolume (10⁵ μm³ mL⁻¹)	7.33 ± 0.02	7.89 ± 0.12**	8.15 ± 0.08**	8.40 ± 0.07	8.71 ± 0.08**	8.92 ± 0.10**	$p < 0.001$
	Mean cell diameter (μm)	5.31 ± 0.01	5.35 ± 0.01**	5.34 ± 0.01*	5.41 ± 0.01	5.41 ± 0.01	5.40 ± 0.01	$p < 0.001$
	Cellular Chl content (pg cell⁻¹)	0.32 ± 0.01	0.33 ± 0.01	0.37 ± 0.01**	0.52 ± 0.01	0.51 ± 0.02	0.50 ± 0.02	$p < 0.001$
	Chl per biovolume (g L⁻¹)	4.06 ± 0.12	4.16 ± 0.13	4.60 ± 0.16**	6.25 ± 0.10	6.13 ± 0.15	6.13 ± 0.23	$p < 0.001$
	F_v/F_m	0.441 ± 0.004	0.450 ± 0.016	0.476 ± 0.017**	0.504 ± 0.000	0.510 ± 0.014	0.511 ± 0.004	$p < 0.001$
	Chl biosynthesis rate (h⁻¹)	0.0248 ± 0.0027	0.0448 ± 0.0037**	0.0502 ± 0.0071**	0.0924 ± 0.0031	0.1054 ± 0.0029**	0.0975 ± 0.0032	$p < 0.001$
	Abundance-based growth rates (h⁻¹)	0.0411 ± 0.0003	0.0461 ± 0.0016**	0.0513 ± 0.0010**	0.0476 ± 0.0012	0.0518 ± 0.0019**	0.0511 ± 0.0025*	$p < 0.001$
	Biovolume-based growth rates (h⁻¹)	0.0385 ± 0.0007	0.0455 ± 0.0012**	0.0507 ± 0.0009**	0.0513 ± 0.0012	0.0578 ± 0.0014**	0.0575 ± 0.0017**	$p < 0.001$
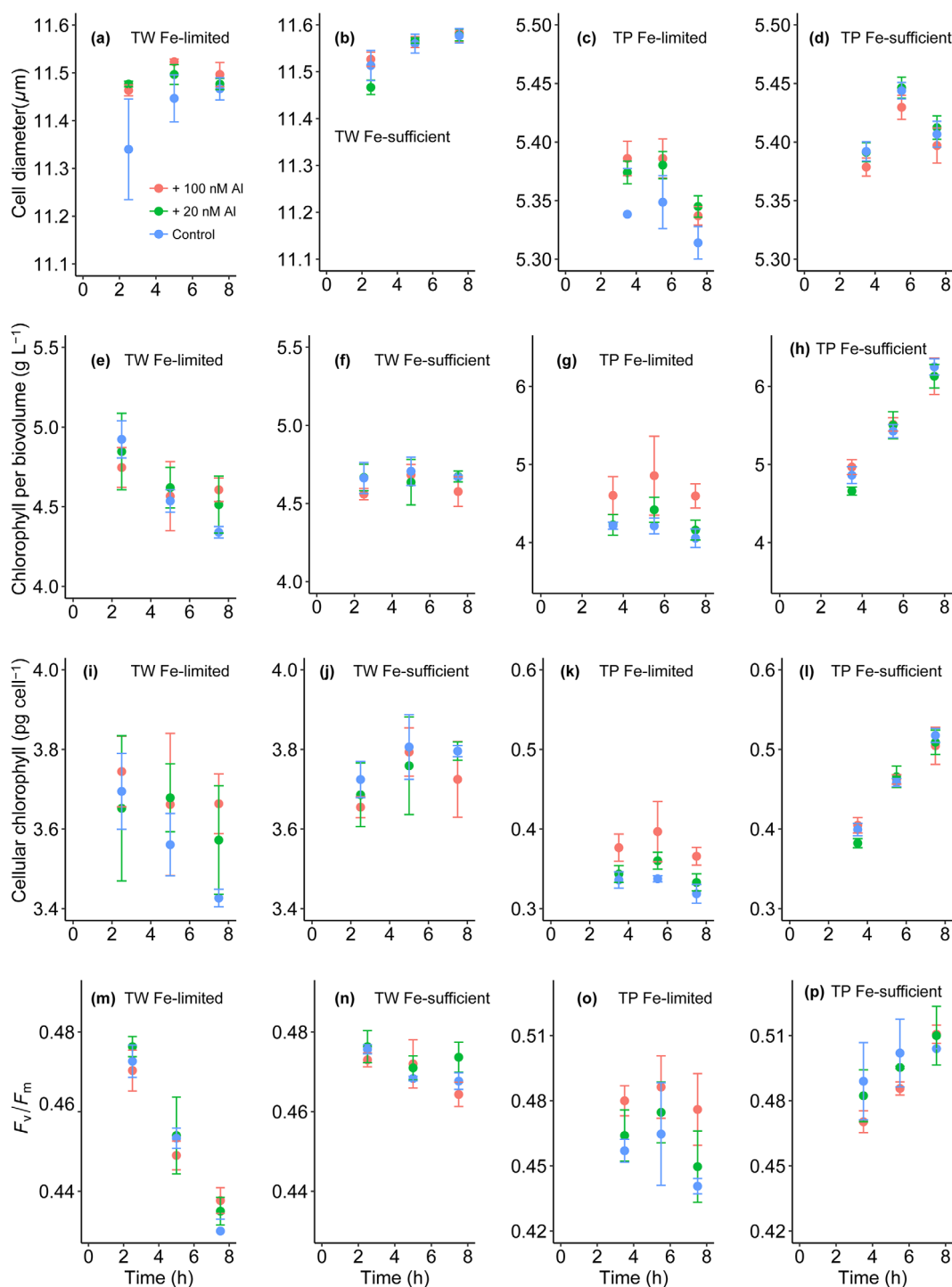
Fig. 4. Effects of aluminum (Al) addition on cellular chlorophyll content and photosynthetic quantum efficiency of two diatoms (*Thalassiosira weissflogii* (TW), and *T. pseudonana* (TP)) in Fe-limited (46 pM [Fe']) and Fe-sufficient (576 pM [Fe']) Aquil* media. The error bars represent standard deviations (n = 3).

(ANOVA, $p = 0.068$), and by 2.0–8.0% for *T. pseudonana* (ANOVA, $p = 0.045$), compared to the control (Fig. 4m,o). In contrast, Al addition under Fe-sufficient conditions did not change the mean cell size, chlorophyll per biovolume, cellular

chlorophyll content, or photosynthetic quantum efficiency (F_v/F_m) for either diatom (ANOVA, $p > 0.1$) (Fig. 4b,d,f,h,j,l,h,p).

Under Fe-limited conditions, the higher cellular chlorophyll content and F_v/F_m values caused by Al addition

occurred earlier for *T. pseudonana* than *T. weissflogii*. For *T. weissflogii*, higher chlorophyll per unit biovolume (Kruskal–Wallis test, $p = 0.061$), cellular chlorophyll content (Kruskal–Wallis test, $p = 0.051$), and F_v/F_m (ANOVA, $p = 0.068$) in the Al-enriched treatments compared to the control were observed only at the final time point of 7.5 h (Fig. 4e,i,m). In contrast, for *T. pseudonana*, the beneficial effects of Al addition on chlorophyll per unit biovolume (ANOVA, $p < 0.05$), cellular chlorophyll content (ANOVA, $p < 0.05$), and F_v/F_m (ANOVA, $p < 0.05$) occurred earlier at 3.5 h of incubation, and the effects remained until the end of the incubation (repeated-measures ANOVA, $p < 0.05$; Mauchly's test of sphericity, $p > 0.05$) (Fig. 4g,k,o).

Effects of Al addition on chlorophyll biosynthesis and diatom growth rates

The results showed that Al addition to Fe-limited media, as well as the increased Fe supply in Fe-sufficient media, significantly increased the chlorophyll biosynthesis and growth rates of diatoms (Fig. 5). Sufficient Fe supply in the Fe-sufficient media compared to the Fe-limited media increased the (in vivo) chlorophyll biosynthesis rate, abundance-based growth rate, and biovolume-based growth rate by 106%
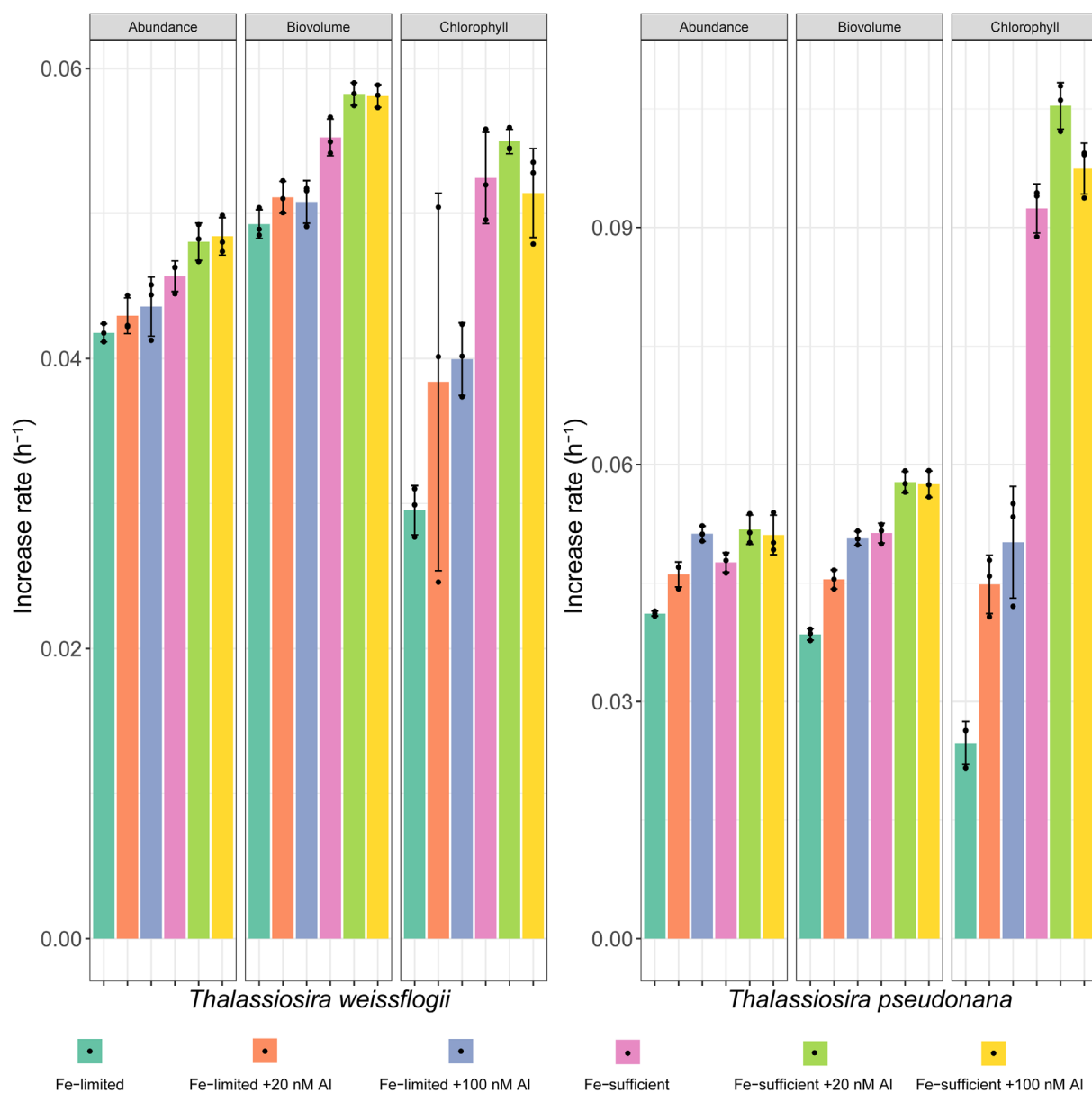

Fig. 5. Effects of aluminum (Al) addition on the growth rates of *T. weissflogii* and *T. pseudonana* in Fe-limited (46 pM [Fe']) and Fe-sufficient (576 pM [Fe']) Aquil* media. Growth rates are expressed in terms of chlorophyll biosynthesis, cell abundance, and biovolume. The error bars represent standard deviations (n = 3).

($p < 0.001$), 9.3% ($p = 0.004$) and 12.2% ($p < 0.001$) for *T. weissflogii*, and 272% ($p < 0.001$), 15.8% ($p < 0.001$), and 33.2% ($p < 0.001$) for *T. pseudonana*, respectively (Table 1).

Aluminum addition to Fe-limited media significantly increased the chlorophyll biosynthesis rate by 45–60% for *T. weissflogii* (ANOVA, $p < 0.05$), and 81–102% for *T. pseudonana* (ANOVA, $p < 0.01$). Aluminum addition to Fe-limited media also increased the abundance-based and biovolume-based growth rates by 2.6–4.3% and 3.0–3.7% for *T. weissflogii* (ANOVA, $p > 0.1$), respectively, and by 12.2–24.7% and 18.2–31.7% for *T. pseudonana* (ANOVA, $p < 0.01$), respectively.

In contrast, Al addition under Fe-sufficient conditions did not significantly change the chlorophyll biosynthesis rates of either diatom (ANOVA, $p > 0.1$), except that the presence of 20 nM Al increased the chlorophyll biosynthesis rate of *T. pseudonana* by 14% ($p < 0.01$). That is to say, the positive effects of Al addition on chlorophyll biosynthesis were not apparent in Fe-sufficient media. However, Al addition in Fe-sufficient media still significantly increased *T. weissflogii* growth rates based on cell abundance (by 5.3–5.9%) (ANOVA, $p = 0.064$), and biovolume (by 5.1–5.3%) (ANOVA, $p = 0.015$). Aluminum addition to Fe-sufficient media also significantly increased *T. pseudonana* growth rates based on cell abundance (by 7.4–8.8%) (ANOVA, $p = 0.08$), biovolume (12.1–12.7%) (ANOVA, $p < 0.01$) (Fig. 5).

Discussion

Our results showed that Al additions at the environmentally relevant levels of 20 and 100 nM to Fe-limited Aquil* media significantly increased the chlorophyll biosynthesis rate, mean cell size, cellular chlorophyll content, and photosynthetic quantum efficiency (F_v/F_m) of the two Fe-limited diatoms (*T. weissflogii* and *T. pseudonana*), and thus their growth rates (Figs. 3–5). To a certain extent, these changes resembled those noted in the diatom grown in the Fe-sufficient medium. Aluminum addition to the Fe-sufficient medium also significantly increased the diatom growth rates, although the beneficial effects on the chlorophyll synthesis rate, mean cell size, cellular chlorophyll content, and photosynthetic quantum efficiency (F_v/F_m) were not apparent. The results also showed that the addition of Al (20 and 100 nM) to our sample of natural seawater had little influence on the concentration of dissolved Fe or Fe solubility (Fig. 1), but decreased the Fe uptake rates of *T. weissflogii* and resulted in slightly lower cellular Fe content under Fe-limited conditions (Fig. 2). These results suggest that the beneficial effects of Al addition were not the result of an increased supply of Fe from seawater. Rather in the presence of Al, Fe-limited diatom cells could reach higher chlorophyll synthesis rates and photosynthetic efficiency with slightly lower cellular Fe content.

If the positive effects were applicable to Fe-limited marine diatoms in the HNLC regions, we speculate that Al fertilization might increase the growth and carbon fixation of Fe-limited diatoms by enhancing chlorophyll synthesis and photosynthetic efficiency in such regions as the Southern Ocean. This study adds new evidence and support for the iron-aluminum hypothesis.

Effects of Al on the photosynthesis and growth of marine phytoplankton

The promoting effects of Al on the growth and carbon fixation of marine phytoplankton have previously been outlined (Zhou et al. 2016, 2018a,b, 2021; Liu et al. 2018). Increased use efficiencies of dissolved organic phosphorus and Fe have been proposed as possible mechanisms for the positive effects (Zhou et al. 2016, 2018b). The present study adds to these considerations and shows that Al addition was beneficial with respect to chlorophyll biosynthesis, cellular chlorophyll content, photosynthetic efficiency, and growth of two marine diatoms under Fe-limited conditions (Table 1). The present study also shows that Al addition increased the growth rates of these marine diatoms in Fe-sufficient media, although it did not significantly change diatom cellular chlorophyll content (Figs. 4, 5).

Previous studies also reported high cellular chlorophyll content and enhanced growth of marine phytoplankton including *T. weissflogii* in seawater media enriched with Al (Shi et al. 2015; Zhou et al. 2016); *f*/2 medium and its derivatives (such as *f*/200) were used in these studies. The nominal concentrations of Fe in the media were deemed to be sufficient for marine phytoplankton growth. However, the use of an equimolar concentration of EDTA to buffer Fe (molar ratio of EDTA : Fe of 1 : 1), and the procedure of sterilization by autoclaving may have led to the precipitation of some of the added Fe as hydrous ferric oxide (Sunda et al. 2005). The precipitation of Fe may lead to poorly constrained Fe availability in the media, and under such conditions, it is unclear if the observed effects of Al addition on the cellular chlorophyll content of marine phytoplankton were related to Fe-limitation.

The present study provides clear evidence showing that Al addition to Fe-limited Aquil* medium increased the chlorophyll biosynthesis rates and cellular chlorophyll content of two diatoms (Figs. 4, 5). The increased chlorophyll biosynthesis and cellular chlorophyll content supported higher photosynthetic efficiency (Fig. 4) and increased the growth rates of the diatoms (Fig. 5). Iron plays roles in chlorophyll biosynthesis (Pushnik et al. 1984; Terry and Abadía 1986; Suehiro et al. 2021; Jiang et al. 2023), and Fe fertilization significantly stimulated chlorophyll increases in Fe-limited HNLC regions (Martin and Fitzwater 1988; Boyd et al. 2000; Strong et al. 2009). Our results showed that Fe deficiency inhibited chlorophyll biosynthesis, cellular chlorophyll content, photosynthetic efficiency, and growth rates of two diatoms in Fe-limited media compared to the Fe-sufficient media (Table 1). Ample Fe supply liberated all the limitations and significantly improved the status of all the variables. Moreover, Al addition

worked in a somewhat similar manner to the increased Fe supply and significantly enhanced the chlorophyll biosynthesis, cellular chlorophyll content, photosynthetic efficiency, and growth rates of two diatoms in Fe-limited media (Supporting Information Fig. S2). In contrast, the promoting effects of Al addition on chlorophyll biosynthesis and cellular chlorophyll content were not apparent in Fe-sufficient media. These results suggested that Al addition had increased Fe bioavailability for chlorophyll biosynthesis. However, the Fe uptake experiments suggest that the increase in Fe bioavailability may have occurred intracellularly.

The influence of Al on Fe bioavailability

The results of the experiments designed to test the influence of Al on the concentration of dissolved Fe (Fe solubility) in seawater and Fe uptake by the marine diatom *T. weissflogii* did not show any indication that the presence of Al increased Fe bioavailability and Fe uptake by this marine diatom. Calculations based on the Visual MINTEQ model indicate that Al addition does not impact the speciation of Fe and the concentrations of dissolved inorganic Fe in seawater and the experimental media (Supporting Information Table S4). Aluminum addition at the levels of 20 and 100 nM did not influence the dissolved Fe concentration (or Fe solubility) as determined in the present experiments (Fig. 1) but did result in decreased Fe uptake rates by the diatom *T. weissflogii* under Fe-limited conditions (Fig. 2; Table 1).

Our results differ from those presented in a study by Santana-Casiano et al. (1997), who reported that in the presence of Al (500 nM), the marine diatom (*T. weissflogii*) took up Fe at significantly higher rates in a seawater medium with 100 nM Fe buffered with 100 nM EDTA. The authors suggested that Al may increase the concentration of labile Fe in seawater. However, the exact mechanisms were unknown. Zhou et al. (2018*a,b*) proposed that Al may increase Fe bioavailability by complexing with superoxide in seawater and catalyzing the extracellular reduction of Fe(III) to Fe(II). This hypothesis was based on the knowledge that extracellular reduction of Fe(III) to Fe(II) is often a prerequisite for Fe uptake by marine phytoplankton, and Al has a significant pro-oxidant activity and can bind with superoxide to form an Al-superoxide complex (Exley 2004; Mujika et al. 2011), which catalyzes the reduction of Fe(III) to Fe(II) in vitro and in vivo (Shaked et al. 2005; Rose 2012; Ruipérez et al. 2012). However, our present results showed that Al addition did not increase but rather decreased the Fe uptake rate of the same marine diatom (*T. weissflogii*) (Fig. 5).

There are two main differences between the present study and the study by Santana-Casiano et al. (1997). First, Santana-Casiano et al. (1997) used 100 nM Fe buffered with 0.1 μM EDTA while we used 47 nM Fe buffered with 100 μM EDTA in the exposure media. This would lead to differences in the concentrations of dissolved inorganic Fe ([Fe′], bioavailable) in the exposure media. The concentration of dissolved inorganic Fe

was several orders of magnitude higher in the study by Santana-Casiano et al. (1997) (> 1 nM [Fe′]) than in the present study (54 pM [Fe′]). In addition, a large fraction (> 50%) of Fe was present in colloidal form in the study by Santana-Casiano et al. (1997). Aluminum may have different influences on the bioavailability of dissolved inorganic Fe and colloidal Fe to marine diatoms. Second, Fe-limited diatom cells were used in the present study, while Fe-replete diatom cells were used in the Santana-Casiano et al. (1997) study. Aluminum addition may have different impacts on the Fe-limited diatom cell and Fe-replete diatom cell. The different experimental designs may yield opposite effects with respect to Al on Fe uptake by the same marine diatom.

We suggest that the artificial ligand EDTA-buffered system may mask the effects of superoxide-facilitated extracellular reduction of Fe(III) to Fe(II), and thus a possible role of Al in increasing Fe bioavailability. Kustka et al. (2005) reported that superoxide indeed can facilitate the extracellular reduction of Fe(III) to Fe(II), but the increased supply of Fe(II) did not change the Fe uptake rate by the marine diatom *T. weissflogii* in a (100 μM) EDTA-buffered Aquil* medium. We used the same high concentration of 100 μM EDTA to buffer Fe in the Aquil* medium.

In our experiments, the Al additions not only failed to increase Fe uptake by *T. weissflogii*, but they also had the opposite effect. The underlying mechanisms for the decreased Fe uptake of *T. weissflogii* in the presence of Al are unclear. Calculations with the Visual MINTEQ chemical equilibrium model (Gustafsson 2020) suggest that the high concentration of 100 μM EDTA will complex the majority (> 99.99%) of the 47 nM Fe, and control the concentrations of dissolved inorganic Fe to pM levels (54 pM). In contrast, EDTA does not complex Al appreciably at seawater pH (Zhou et al. 2016) (Supporting Information Table S5). As a result, the concentrations of dissolved inorganic Al (i.e., 20 and 100 nM) could be three orders of magnitude higher than that of dissolved inorganic Fe in the 100 μM EDTA-buffered Aquil* medium. Note that at these Al concentrations, the ion activity product for $Al(OH)_3(s)$ is more than seven orders of magnitude below the solubility limit as calculated for the most likely initial aluminum hydroxide solid, microcrystalline Gibbsite (Hem and Roberson 1967). Our previous study showed that the marine diatom *T. weissflogii* could assimilate Al from seawater, and the Al uptake rate by *T. weissflogii* was comparable to the Fe uptake rates by the same marine diatom when dissolved Fe in seawater was present at a level of about 100 nM and was not buffered by strong organic ligands (Anderson and Morel 1982; Liu et al. 2019). However, the Al uptake mechanisms are still unknown. The present results inspire us to suggest that some of the Al might be absorbed by the marine diatom through a Fe(III) uptake transporter (Sutak et al. 2020). The high concentrations (20 and 100 nM) of dissolved inorganic Al might compete with a low concentration of dissolved inorganic Fe(III) (i.e., 54 pM) for binding at the uptake site, resulting in

decreased Fe uptake rates by the marine diatom in the present study. Further work is needed to follow up on this speculation.

In light of the foregoing reasoning, we suggest that the EDTA-buffered system may not be suitable for testing the hypothesis that Al complexes with superoxide and catalyzes the reduction of Fe(III) to Fe(II) in vitro (Zhou et al. 2018*b*). The use of EDTA was a major advance in algal culturing and aided the study and understanding of trace metal uptake, limitation, and toxicity (Sunda et al. 2005). However, such strong ligand concentrations are not found in natural seawater, and we must re-examine the risks of generating possibly misleading results by using high concentrations of EDTA in culture media. In our view, the present study results do not justify the rejection of the hypothesis that Al may complex with superoxide and under certain conditions catalyze the reduction of Fe(III) to Fe(II) in vitro. We believe that it would be worthwhile to check directly whether Al could facilitate the reduction of Fe(III) to Fe(II) in seawater by using Ferrozine and ^{55}Fe labeling methods as suggested by Kustka et al. (2005).

Possible mechanisms underlying the promoting effects of Al on chlorophyll biosynthesis and diatom growth

The present Fe uptake experiments indicated that Al could decrease marine diatom Fe uptake rates and yet allow the diatom *T. weissflogii* to achieve higher chlorophyll biosynthesis and growth rates in Fe-limited media (Figs. 2, 5). That is to say, the promoting effects of Al on chlorophyll biosynthesis under Fe-limited conditions were not related to increased Fe supply from seawater. Rather, our results suggest that Al may enhance chlorophyll biosynthesis by improving the use efficiency of cellular Fe.

Our results showed that Fe-limited diatom (*T. weissflogii*) cells in the Al-enriched treatments achieved higher chlorophyll biosynthesis rates with lower cellular Fe content than did the control treatments in the absence of added Al (Fig. 5; Table 1). However, the Al-induced increases in cellular chlorophyll content, chlorophyll biosynthesis rate, and photosynthetic quantum efficiency (F_v/F_m) were lower than those induced by the supply of sufficient Fe (Supporting Information Fig. S2). Our results also showed that the positive effects of Al on cellular chlorophyll content, and chlorophyll biosynthesis disappeared under Fe-sufficient conditions (Figs. 4, 5; Table 1). These results suggest that the Al-induced increase in chlorophyll biosynthesis rate of diatoms under Fe-limited conditions was related in some manner to Fe scarcity. Nevertheless, as discussed above, the lower Fe uptake rates of the diatom in the Al-enriched treatments (Fig. 2; Supporting Information Fig. S1) suggest that the effects of Al addition were not a result of enhanced Fe supply (uptake) from seawater to the cell. Rather they suggest that in the presence of Al, lower cellular Fe could support higher chlorophyll biosynthesis rates. Therefore, we speculate that Al may enhance chlorophyll

biosynthesis by influencing the use of cellular Fe and support higher chlorophyll biosynthesis rates. Given that Fe(II) is needed in the pathway of chlorophyll biosynthesis (Suehiro et al. 2021; Jiang et al. 2023), one possible manner is that Al may help maintain more cellular Fe in Fe(II) form by facilitating the superoxide-mediated intracellular reduction of Fe(III) to Fe(II) (Exley 2004; Mujika et al. 2011; Ruipérez et al. 2012).

It should be pointed out that no established biological role of Al has been found yet (Exley and Mold 2015) and the present study did not prove any biological role for Al. Aluminum's apparent lack of an essential biological role despite its wide presence in the environment and biological systems is puzzling (Exley 2013). This paradox has stimulated continuous efforts to explore the possible biological role of Al (Exley and Mold 2015; Sun et al. 2020), especially in the Aluminum Age when biota are experiencing a burgeoning exposure to biologically available Al (Exley 2003; Exley and Mold 2015). The present study inspires us to ask a question that may be linked to the possible biological role of Al: Could Al enhance the use of cellular Fe by facilitating the superoxide-mediated intracellular reduction of Fe(III) to Fe(II)? No doubt further work to answer the question is needed to examine the possible role of Al in the biosynthesis of chlorophyll in marine diatoms.

Implications for the carbon cycle in the HNLC oceans

The present study suggests that Al addition at environmentally relevant levels could increase the chlorophyll biosynthesis and growth (carbon fixation) of marine diatoms, especially under Fe-limited conditions. This is a new aspect of the possible indirect roles of Al in influencing growth and carbon fixation by marine phytoplankton. The present study adds new evidence for the iron–aluminum hypothesis (Zhou et al. 2018*b*), which proposes that Al, as well as Fe, may play an important role in the glacial–interglacial climate cycles because Al could influence carbon fixation in the upper ocean by increasing the use of dissolved organic phosphorus, Fe, and dinitrogen.

Based on the present study, one might also speculate that natural/artificial Al fertilization might increase the growth and carbon fixation of Fe-limited diatoms by enhancing chlorophyll synthesis and photosynthetic efficiency. This may be relevant to HNLC regions such as the Southern Ocean, provided that the promoting effects of Al were applicable to marine diatoms in these regions. We suggest that the inputs of Al to the ocean through dust deposition, river discharge, hydrothermal venting, and sediment resuspension could work on their own or together with Fe in enhancing the chlorophyll biosynthesis and photosynthetic efficiency of marine phytoplankton in Fe-limited HNLC regions. Further laboratory work using native diatom species from the HNLC regions is needed to test the reproducibility of the positive effects of Al on diatom chlorophyll biosynthesis and growth. Onboard incubation experiments in the HNLC regions are also needed to test the effects of Al addition on the chlorophyll

biosynthesis and growth of marine phytoplankton. After that, further mesoscale fertilization experiments involving the addition of Al alone or Fe and Al together in HNLC regions such as the Southern Ocean might be needed to test the potential CO_2 removal efficiency and environmental impacts of Al and Fe fertilization.

Conclusion

This study reports the promoting effects of Al on the chlorophyll biosynthesis and growth of two marine diatoms under Fe-limited conditions. It provides a new perspective on the possible roles of Al in influencing the growth and carbon fixation by marine phytoplankton. Our results also showed that the positive effects were not a result of increased Fe bioavailability from seawater to the phytoplankton cell. Rather, in the presence of Al diatoms achieved higher chlorophyll biosynthesis rates with less cellular Fe content under Fe-limited conditions. We speculate that Al might enhance chlorophyll biosynthesis indirectly by influencing the use of cellular Fe via facilitating the intracellular superoxide-mediated reduction of Fe(III) to Fe(II). Although Al does not play any biological role, its indirect involvement in nutrient acquisition and/or management warrants further investigation.

Data availability statement

Data for this manuscript are available at the South China Sea Ocean Data Center, National Earth System Science Data Center, National Science and Technology Infrastructure of China (http://data.scsio.ac.cn/metaData-detail/1692345741134483456).

References

Anderson, M. A., and F. M. M. Morel. 1982. The influence of aqueous iron chemistry on the uptake of iron by the coastal diatom *Thalassiosira weissflogii*. Limnol. Oceanogr. **27**: 789–813. doi:10.4319/lo.1982.27.5.0789

Anderson, R. P., and others. 2020. Aluminosilicate haloes preserve complex life approximately 800 million years ago. Interf. Focus **10**: 20200011. doi:10.1098/rsfs.2020.0011

Blain, S., and others. 2007. Effect of natural iron fertilization on carbon sequestration in the Southern Ocean. Nature **446**: 1070–1074. doi:10.1038/nature05700

Blattmann, T. M., and others. 2019. Mineralogical control on the fate of continentally derived organic matter in the ocean. Science **366**: 742–745. doi:10.1126/science.aax5345

Boyd, P. W., and others. 2000. A mesoscale phytoplankton bloom in the polar Southern Ocean stimulated by iron fertilization. Nature **407**: 695–702. doi:10.1038/35037500

Boyd, P. W., and others. 2007. Mesoscale iron enrichment experiments 1993–2005: Synthesis and future directions. Science **315**: 612–617. doi:10.1126/science.1131669

Browning, T. J., and C. M. Moore. 2023. Global analysis of ocean phytoplankton nutrient limitation reveals high prevalence of co-limitation. Nat. Commun. **14**: 5014. doi:10.1038/s41467-023-40774-0

de Baar, H. J., L. J. Gerringa, P. Laan, and K. R. Timmermans. 2008. Efficiency of carbon removal per added iron in ocean iron fertilization. Mar. Ecol. Prog. Ser. **364**: 269–282. doi:10.3354/meps07548

Dixit, S., P. Van Cappellen, and A. J. van Bennekom. 2001. Processes controlling solubility of biogenic silica and pore water build-up of silicic acid in marine sediments. Mar. Chem. **73**: 333–352. doi:10.1016/S0304-4203(00)00118-3

Exley, C. 2003. A biogeochemical cycle for aluminium? J. Inorg. Biochem. **97**: 1–7. doi:10.1016/S0162-0134(03)00274-5

Exley, C. 2004. The pro-oxidant activity of aluminum. Free Radic. Biol. Med. **36**: 380–387. doi:10.1016/j.freeradbiomed.2003.11.017

Exley, C. 2013. Aluminum in biological systems, p. 33–34. *In* R. H. Kretsinger, V. N. Uversky, and E. A. Permyakov [eds.], Encyclopedia of metalloproteins. Springer. doi:10.1007/978-1-4614-1533-6_105

Exley, C., and M. J. Mold. 2015. The binding, transport and fate of aluminium in biological cells. J. Trace Elem. Med. Biol. **30**: 90–95. doi:10.1016/j.jtemb.2014.11.002

Friedlingstein, P., and others. 2022. Global carbon budget 2021. Earth Syst. Sci. Data **14**: 1917–2005. doi:10.5194/essd-14-1917-2022

GESAMP, and others. 2019. High level review of a wide range of proposed marine geoengineering techniques, p. 144. *In* P. Boyd and C. M. G. Vivian [eds.]. IMO/FAO/UNESCO-IOC/UNIDO/WMO/IAEA/UN/UN Environment/UNDP/ISA Joint Group of Experts on the Scientific Aspects of Marine Environmental Protection. Rep. Stud. GESAMP No. 98.

Gustafsson, J. P. 2020. Visual MINTEQ version 3.1. KTH Royal Institute of Technology, Department of Land and Water Resources Engineering, Available from: https://vminteq.lwr.kth.se/

Hem, J. D., and C. E. Roberson. 1967. Form and stability of aluminum hydroxide complexes in dilute solution. Geological Survey Water Supply Paper Series 1827 A. p. 55. U.S. Government Publishing Office. doi:10.3133/wsp1827A

Hemingway, J. D., and others. 2019. Mineral protection regulates long-term global preservation of natural organic carbon. Nature **570**: 228–231. doi:10.1038/s41586-019-1280-6

IPCC. 2022. Climate change 2022: Mitigation of climate change. *In* P. R. Shukla, and others [ed.] Contribution of Working Group III to the Sixth Assessment Report of the Intergovernmental Panel on Climate Change. Cambridge University Press. doi:10.1017/9781009157926.001

Jabre, L., and E. M. Bertrand. 2020. Interactive effects of iron and temperature on the growth of *Fragilariopsis cylindrus*. Limnol. Oceanogr. Lett. **5**: 363–370. doi:10.1002/lol2.10158

Jiang, Y., T. Cao, Y. Yang, H. Zhang, J. Zhang, and X. Li. 2023. A chlorophyll c synthase widely co-opted by phytoplankton. Science **382**: 92–98. doi:10.1126/science.adg7921

Kustka, A. B., Y. Shaked, A. J. Milligan, D. W. King, and F. M. Morel. 2005. Extracellular production of superoxide by marine diatoms: Contrasting effects on iron redox chemistry and bioavailability. Limnol. Oceanogr. **50**: 1172–1180. doi:10.4319/lo.2005.50.4.1172

Lewin, J. C. 1961. The dissolution of silica from diatom walls. Geochim. Cosmochim. Acta **21**: 182–198. doi:10.1016/S0016-7037(61)80054-9

Liu, J., L. Zhou, G. Li, Z. Ke, R. Shi, and Y. Tan. 2018. Beneficial effects of aluminum enrichment on nitrogen-fixing cyanobacteria in the South China Sea. Mar. Pollut. Bull. **129**: 142–150. doi:10.1016/j.marpolbul.2018.02.011

Liu, J., C. Robinson, D. Wallace, L. Legendre, and N. Jiao. 2022. Ocean negative carbon emissions: A new UN Decade program. Innovation **3**: 100302. doi:10.1016/j.xinn.2022.100302

Liu, Q., and others. 2019. Uptake and subcellular distribution of aluminum in a marine diatom. Ecotoxicol. Environ. Saf. **169**: 85–92. doi:10.1016/j.ecoenv.2018.10.095

Martin, J. H. 1990. Glacial-interglacial CO_2 change: The iron hypothesis. Paleoceanography **5**: 1–13. doi:10.1029/PA005i001p00001

Martin, J. H., and S. E. Fitzwater. 1988. Iron deficiency limits phytoplankton growth in the north-east Pacific subarctic. Nature **331**: 341–343. doi:10.1038/331341a0

Martin, J. H., S. E. Fitzwater, and R. M. Gordon. 1990. Iron deficiency limits phytoplankton growth in Antarctic waters. Global Biogeochem. Cycl. **4**: 5–12. doi:10.1029/GB004i001p00005

Martin, P., and others. 2013. Iron fertilization enhanced net community production but not downward particle flux during the Southern Ocean iron fertilization experiment LOHAFEX. Global Biogeochem. Cycl. **27**: 871–881. doi:10.1002/gbc.20077

Moore, C. M., and others. 2013. Processes and patterns of oceanic nutrient limitation. Nat. Geosci. **6**: 701–710. doi:10.1038/ngeo1765

Mujika, J. I., F. Ruipérez, I. Infante, J. M. Ugalde, C. Exley, and X. Lopez. 2011. Pro-oxidant activity of aluminum: Stabilization of the aluminum superoxide radical ion. J. Phys. Chem. A **115**: 6717–6723. doi:10.1021/jp203290b

Pollard, R. T., and others. 2009. Southern Ocean deep-water carbon export enhanced by natural iron fertilization. Nature **457**: 577–580. doi:10.1038/nature07716

Pushnik, J. C., G. W. Miller, and J. H. Manwaring. 1984. The role of iron in higher plant chlorophyll biosynthesis, maintenance and chloroplast biogenesis. J. Plant Nutr. **7**: 733–758. doi:10.1080/01904168409363238

R Core Team. 2023. R: A language and environment for statistical computing. R Foundation for Statistical Computing, Available from https://www.R-project.org/

Rose, A. L. 2012. The influence of extracellular superoxide on iron redox chemistry and bioavailability to aquatic microorganisms. Front. Microbiol. **3**: 124. doi:10.3389/fmicb.2012.00124

Ruipérez, F., J. I. Mujika, J. M. Ugalde, C. Exley, and X. Lopez. 2012. Pro-oxidant activity of aluminum: Promoting the Fenton reaction by reducing Fe(III) to Fe(II). J. Inorg. Biochem. **117**: 118–123. doi:10.1016/j.jinorgbio.2012.09.008

Santana-Casiano, J. M., M. Gonzalez-Davila, L. M. Laglera, J. Perez-Pena, L. Brand, and F. J. Millero. 1997. The influence of zinc, aluminum and cadmium on the uptake kinetics of iron by algae. Mar. Chem. **59**: 95–111. doi:10.1016/s0304-4203(97)00068-6

Shaked, Y., A. B. Kustka, and F. M. Morel. 2005. A general kinetic model for iron acquisition by eukaryotic phytoplankton. Limnol. Oceanogr. **50**: 872–882. doi:10.4319/lo.2005.50.3.0872

Shi, R., G. Li, L. Zhou, and Y. Tan. 2015. Increasing aluminum alters the growth, cellular chlorophyll *a* and oxidation stress of cyanobacteria *Synechococcus* sp. Oceanol. Hydrobiol. Stud. **44**: 343–351. doi:10.1515/ohs-2015-0033

Stoffyn, M. 1979. Biological control of dissolved aluminum in seawater: Experimental evidence. Science **203**: 651–653. doi:10.1126/science.203.4381.651

Strong, A. L., J. J. Cullen, and S. W. Chisholm. 2009. Ocean fertilization science, policy, and commerce. Oceanography **22**: 236–261. doi:10.5670/oceanog.2009.83

Suehiro, H., R. Tanaka, and H. Ito. 2021. Distribution and functional analysis of the two types of 8-vinyl reductase involved in chlorophyll biosynthesis in marine cyanobacteria. Arch. Microbiol. **203**: 3565–3575. doi:10.1007/s00203-021-02348-w

Sun, L., and others. 2020. Aluminum is essential for root growth and development of tea plants (*Camellia sinensis*). J. Integr. Plant Biol. **62**: 984–997. doi:10.1111/jipb.12942

Sunda, W., and S. Huntsman. 2003. Effect of pH, light, and temperature on Fe–EDTA chelation and Fe hydrolysis in seawater. Mar. Chem. **84**: 35–47. doi:10.1016/S0304-4203(03)00101-4

Sunda, W. G., N. M. Price, and F. M. M. Morel. 2005. Trace metal ion buffers and their use in culture studies, p. 35–63. *In* R. A. Andersen [ed.], Algal culturing techniques. Academic Press.

Sutak, R., J. M. Camadro, and E. Lesuisse. 2020. Iron uptake mechanisms in marine phytoplankton. Front. Microbiol. **11**: 566691. doi:10.3389/fmicb.2020.566691

Terry, N., and J. Abadía. 1986. Function of iron in chloroplasts. J. Plant Nutr. **9**: 609–646. doi:10.1080/01904168609363470

Tian, Q., D. Liu, M. Li, P. Yuan, J. Zhou, and H. Guo. 2023. Increasing iron concentration inhibits the Al-incorporation into the diatom biogenic silica: From laboratory simulation of ocean iron fertilization. Chem. Geol. **639**: 121713. doi:10.1016/j.chemgeo.2023.121713

Tovar-Sanchez, A., S. A. Sañudo-Wilhelmy, M. Garcia-Vargas, R. S. Weaver, L. C. Popels, and D. A. Hutchins. 2003. A trace metal clean reagent to remove surface-bound iron

from marine phytoplankton. Mar. Chem. **82**: 91–99. doi:10.1016/S0304-4203(03)00054-9

Yoon, J. E., and others. 2018. Reviews and syntheses: Ocean iron fertilization experiments—Past, present, and future looking to a future Korean Iron Fertilization Experiment in the Southern Ocean (KIFES) project. Biogeosciences **15**: 5847–5889. doi:10.5194/bg-15-5847-2018

Zhou, L., Y. Tan, L. Huang, and W.-X. Wang. 2016. Enhanced utilization of organic phosphorus in a marine diatom *Thalassiosira weissflogii*: A possible mechanism for aluminum effect under P limitation. J. Exp. Mar. Biol. Ecol. **478**: 77–85. doi:10.1016/j.jembe.2016.02.009

Zhou, L., J. Liu, S. Xing, Y. Tan, and L. Huang. 2018*a*. Phytoplankton responses to aluminum enrichment in the South China Sea. J. Inorg. Biochem. **181**: 117–131. doi:10.1016/j.jinorgbio.2017.09.022

Zhou, L., Y. Tan, L. Huang, C. Fortin, and P. G. C. Campbell. 2018*b*. Aluminum effects on marine phytoplankton: Implications for a revised iron hypothesis (iron–aluminum hypothesis). Biogeochemistry **139**: 123–137. doi:10.1007/s10533-018-0458-6

Zhou, L., and others. 2021. Aluminum increases net carbon fixation by marine diatoms and decreases their decomposition: Evidence for the iron–aluminum hypothesis. Limnol. Oceanogr. **66**: 2712–2727. doi:10.1002/lno.11784

Zhou, L., L. Huang, and Y. Tan. 2023*a*. Iron-aluminum hypothesis and the potential of ocean aluminum fertilization as a carbon dioxide removal strategy (in Chinese with English abstract). J. Trop. Oceanogr. **42**: 1–18. doi:10.11978/2022153

Zhou, L., F. Liu, Y. Tan, C. Fortin, L. Huang, and P. G. C. Campbell. 2023*b*. Aluminum-induced changes in the net carbon fixation and carbon decomposition of a nitrogen-fixing cyanobacterium *Trichodesmium erythraeum*. Biogeochemistry **165**: 277–290. doi:10.1007/s10533-023-01081-4

Conflict of Interest

None declared.

Submitted 06 September 2023
Revised 10 March 2024
Accepted 17 March 2024

Associate editor: Katherina Petrou